Radiation of Plane Structures at High Frequency Using an Energy Method

V. Cotoni and A. Le Bot

Laboratoire de Tribologie et Dynamique des Systemes, Ecole Centrale de Lyon - 36, av Guy de Collongue, BP 163, 69131 Ecully cedex, France

(Received 5 October 1999; accepted 7 June 2001)

This paper is concerned with the calculation, by means of an energy approach, of the acoustic radiation from plane structures where the flexural waves are supersonic. The structural deflections and acoustic pressure fields are described in terms of local energy quantities, according to the so-called energy flow method. Some local power balance equations governing the energy propagation inside each subsystem and energy transfers at the couplings are solved, leading to the spatial description of the energy fields inside each subsystem. This theoretical analysis is focused on the simple case of a baffled point-excited beam radiating in a two-dimensional semi-infinite acoustic medium. Comparisons with results from the numerical solution of equations of motion show good agreement for high frequencies and demonstrate the ability of the energy flow method to predict the pattern of non-diffuse radiated sound fields.

1. INTRODUCTION

This paper deals with the calculation of vibroacoustic systems at high frequency. Classical approaches for the numerical solution of governing equations like the finite element method become rapidly inefficient as frequency increases due to the great number of degrees of freedom. In addition, the response of systems becomes very sensitive to frequency, geometrical and material parameters, and classical approaches give unnecessarily accurate results while the prediction of the averaged behaviour should be robust and representative enough. In this context, the Statistical Energy Analysis (SEA) approach is intended for vibroacoustic calculations in the high frequency region.[1,2] Assuming that energy fields are diffuse in each subsystem, SEA gives a frequency-averaged response of the subsystems by solving global energy balances.

As an alternative to SEA, the energy flow approach addressed in this paper is able to predict the spatial repartition of energy inside each subsystem and the diffuse field assumption is not necessary anymore. Using local energy quantities and local energy balances, this approach has been developed successfully for assembled plates[3,4] and for acoustic cavities[5-7]. More recently the approach has been applied to the coupling between plates and acoustic cavities where energy fields are reverberant enough.[8,9] The aim of the present study is to develop the coupling between structures and exterior acoustic media where energy fields are not diffuse at all.

Firstly, energy propagation inside subsystems is discussed in Section 2. The second step of the energy flow method is the derivation of the radiation conditions for the vibroacoustic coupling. This is detailed in Section 3 for the simple case of a beam radiating into a two-dimensional semi-infinite acoustic medium. In Section 4, comparisons of the numerical solution of energy flow equations and equations of motion are performed.

2. ENERGY PROPAGATION BY THE ENERGY FLOW METHOD

The energy propagation inside subsystems is first addressed without considering any coupling. It is dealt with according to the following hypothesis. First, systems are linear, isotropic and in steady state conditions at frequency ω. Then, vibration fields are thought of as the superposition of elementary travelling waves. These waves are assumed to be plane, cylindrical or spherical waves, depending on the dimension of the subsystem. Finally, interference between these waves is not taken into account. This means that waves are uncorrelated, making their energy contributions additive. This study has been already done in Refs.[5,6] and is just summarised here. Let us remark that the superposition of travelling waves means that energy fields are incorrectly described near discontinuities where near-field terms may arise.

The first step of the method consists in determining the way in which the energy propagates in these travelling waves. We assume that the local energy balance applied to an elementary volume of the system is given by

$$div\,\mathbf{H} + P_{diss} = \delta_S \,, \tag{1}$$

where $\mathbf{H}$ denotes the intensity vector corresponding to a single travelling wave, P_{diss} the power being dissipated in the volume and δ_S is the Dirac symbol for unit injected power at the source point S. The well-known SEA damping equation, $P_{diss} = \eta\omega G$, where G denotes the energy density and η the damping loss factor, is used to express the power being dissipated. The relation for travelling waves, $\mathbf{H} = cG\,\mathbf{u}$, where c is the energy velocity of waves and $\mathbf{u}$ the unit vector in the direction of propagation is used to express the divergence of $\mathbf{H}$ in the radial co-ordinate r centred in S. By virtue of the radial symmetry, only the radial component of $\mathbf{H}$ is to be considered and one obtains for a system of dimension n,

$$div\,\mathbf{H} = \frac{1}{r^{n-1}}\frac{d}{dr}(r^{n-1}cG) \,. \tag{2}$$

This leads to the solutions for G and $\mathbf{H}$,

$$G(S,M) = \frac{1}{\gamma_0 c}\frac{e^{-\eta\omega r/c}}{r^{n-1}} \quad \text{and} \quad \mathbf{H}(S,M) = \frac{1}{\gamma_0}\frac{e^{-\eta\omega r/c}}{r^{n-1}}\mathbf{u} \,, \tag{3}$$

where γ_0 denotes the solid angle of the space and $r = \overline{SM}$ is the distance between the source point S and the observation

point M. In the example studied in this paper, the beam is described with plane waves ($n=1, \gamma_0=2$) and the two-dimensional acoustic medium with cylindrical waves ($n=2$, $\gamma_0=2\pi$).

Starting with these elementary energy solutions, the total energy density at any point M of the system, $W(M)$, and the corresponding intensity vector $\mathbf{I}(M)$ are built by summing the uncorrelated energy contributions of direct sources $\rho(S)$ located inside the system $S \in \Omega$, and some diffracted sources $\sigma(P)$ located at the boundary of the system $P \in \partial\Omega$,

$$W(M) = \int_{\Omega} \rho(S) G(S,M) dS + \int_{\partial\Omega} \sigma(P, \mathbf{u}_{PM}) G(P,M) dP \; ; \quad (4)$$

$$\mathbf{I}(M) = \int_{\Omega} \rho(S) \mathbf{H}(S,M)\, dS + \int_{\partial\Omega} \sigma(P, \mathbf{u}_{PM})\, \mathbf{H}(P,M) dP \; , \quad (5)$$

where $\mathbf{u}_{SM}$ (respectively $\mathbf{u}_{PM}$) is the unit vector in the direction from the emanating point S (respectively P) to the observation point M.

Source magnitudes ρ are assumed to be known while source magnitudes σ are to be determined by expressing suitable coupling conditions at the boundaries. These coupling conditions are derived in terms of power balances involving local energy quantities from both parts of the coupling. By virtue of the locality principle valid at high frequency,[10] the appropriate power balances are derived by considering the vicinity of couplings only, which often considerably simplifies the resolutions. Resulting canonical solutions are then used to solve the complete system. The canonical problem describing the radiation process above the critical frequency is derived in the next section, and applied to the case of a beam radiating sound into a two-dimensional semi-infinite medium.

3. COUPLING BETWEEN A BEAM AND AN ACOUSTIC MEDIUM

Consider a fluid-loaded beam, excited by a point force at the frequency ω. Since energy fields can be thought of as the superposition of travelling waves, we first deal with the case of a simple travelling flexural wave on the beam.

3.1. Travelling Wave in the Fluid-loaded Beam

The Euler-Bernoulli equation which applies for the transverse beam displacement $u(x)$ under harmonic excitation is $(\nabla^4 - k_s^4) u(x) = p(x,0)/D$, where $k_s = (m_s\omega^2/D)^{1/4}$ is the in vacuo flexural wavenumber with m_s the mass per unit length and D the bending stiffness of the beam. The structural loss factor η_s is introduced by considering the complex stiffness $D \leftarrow D(1+j\eta_s)$. p is the acoustic pressure verifying the Helmholtz equation, $(\Delta + k_a^2) p(x,z) = 0$, where $k_a = \omega/c_a$ is the acoustic wavenumber with c_a being the velocity of sound.

The acoustic medium is assumed to be undamped and k_a is consequently real-valued. The coupling condition between the beam and the fluid requires the equality of normal velocities on the beam, $\partial p(x,0)/\partial z = m_a \omega^2 u(x)$, where m_a denotes the mass per unit volume of the fluid. We denote the fluid-loaded flexural wavenumber by k. Substitution of a propagating displacement $u(x) = u_0 e^{-jkx}$ and the related pressure $p(x,z) = p_0 e^{-jkx - j(k_a^2 - k^2)^{1/2} z}$ (see Fig. 1 for the notation) into previous equations leads to the dispersion equation in k,

$$(k_s^4 - k^4) = j \frac{m_a}{m_s} k_s^4 (k_a^2 - k^2)^{-1/2}. \quad (6)$$

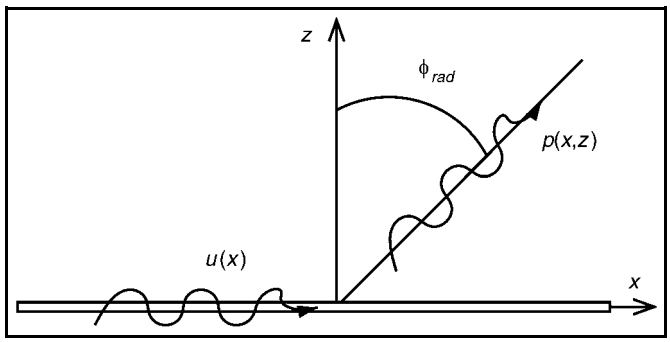

Figure 1. Radiation of a single travelling flexural wave.

This well known equation has five roots.[11,12] Under heavy fluid loading, the distinction between travelling and evanescent waves is not clear and we shall limit our study to light fluid loading. In this case, two solutions of Eq. (6) are near field roots. One is a travelling subsonic root called a *surface wave* and two are subsonic or supersonic travelling roots. Since our energy fields are built with travelling wave contributions, evanescent solutions are not to be considered here. The last two roots are closed to the in vacuo flexural wavenumber k_s when the fluid loading is light, and only one is physically acceptable due to the sign of their imaginary parts. Finally, the surface wave solution that is closed to the acoustic wavenumber does not radiate any power since the corresponding wave in the fluid exponentially decreases with z. Furthermore, under light fluid loading, its contribution to the structural energy is expected to be negligible compared to that of the other acceptable travelling waves. The surface wave is consequently neglected in the following analysis. Only one solution, called a *leaky wave* when it is supersonic, is thus studied.

According to the propagating form of the pressure $p_0 e^{-jkx - j(k_a^2 - k^2)^{1/2} z}$, the acoustic wave is radiated in the direction defined by the angle ϕ_{rad} with the normal to the beam (see Fig. 1)

$$\phi_{rad} = \arcsin\left[\frac{\boldsymbol{R}(k)}{k_a}\right], \quad (7)$$

with $\boldsymbol{R}$ being the real part. The radiated acoustic wave propagates only when $k_a > \boldsymbol{R}(k)$, implying that the flexural waves are supersonic. This occurs when the frequency is above the critical frequency $\omega_c \sim c_a^2 (m_s/D)^{1/2}$ of the fluid-loaded beam. We now focus on systems above the critical frequency.

The time-averaged intensity carried by the radiated wave can be written

$$\mathbf{I}_a(x,z) = \frac{1}{2} \boldsymbol{R}[p(x,z) \mathbf{v}^*(x,z)] =$$

$$\frac{p_0^2}{2 m_a \omega} \boldsymbol{R}[k\mathbf{x} + (k_a^2 - k^2)^{1/2} \mathbf{z}] e^{2\boldsymbol{I}(k)x + 2\boldsymbol{I}(k_a^2 - k^2)^{1/2} z}, \quad (8)$$

where $\mathbf{v} = \mathbf{grad}(p/jm_a\omega)$ denotes the velocity of the fluid, * the complex conjugate and $\boldsymbol{I}$ the imaginary part. The radiated power P_{rad} is the component of $\mathbf{I}_a$ normal to the beam (at $z=0$),

$$P_{rad}(x) = \frac{p_0^2}{2 m_a \omega} \boldsymbol{R}[(k_a^2 - k^2)^{1/2}] e^{2\boldsymbol{I}(k)x}. \quad (9)$$

The time-averaged total energy density W_s of the flexural wave is assumed to be twice the kinetic energy density, $W_s(x) = \frac{1}{2} m_s \omega^2 u_0^2 e^{2I(k)x}$. Using the coupling condition, $m_a \omega^2 u_0 = -j(k_a^2 - k^2)^{1/2} p_0$, the radiated power is expressed in terms of the energy density of the flexural wave,

$$P_{rad}(x) = \frac{m_a}{m_s} \omega \boldsymbol{R}[(k_a^2 - k^2)^{-1/2}] W_s(x) . \qquad (10)$$

The magnitude of the boundary sources σ involved in the acoustic medium description following Eqs. (4) and (5) is given by P_{rad}. Their directivity is given by the angle ϕ_{rad} in Eq. (7). Equation (10) shows that at any point of the x, a part of the flexural intensity is radiated. Consequently, the power balance Eq. (1) for the fluid-loaded beam becomes $div\mathbf{H} + P_{diss} + P_{rad} = \delta_S$. Expressed in terms of loss factors and energy density, one obtains $div\mathbf{H} + (\eta_s + \eta_{rad})\omega W_s = \delta_S$, where η_s is the damping loss factor of the beam and η_{rad} the radiation loss factor given by

$$\eta_{rad} = \frac{m_a}{m_s} \boldsymbol{R}[(k_a^2 - k^2)^{-1/2}] . \qquad (11)$$

Above the critical frequency, fluid coupling effects on flexural waves appear like damping with a loss factor η_{rad}.

3.2. Energy Description of the Coupled System

Consider a simply-supported beam of length l excited at the abscissa point x_0 by a transverse force, and radiating in a semi-infinite acoustic medium. Since there is a single driving point, the first term of Eq. (4) (respectively Eq. (5)) is $\rho_0/2\, G_s(x_0, x)$ (respectively $\rho_0/2\, \mathbf{H}_s(x_0, x)$). In addition, since the beam is one-dimensional, integrals over $\partial\Omega$ reduce to a sum of two terms. The energy density W_s in the beam and the corresponding intensity vector $\mathbf{I}_s$ become

$$\begin{cases} W_s(x) = \dfrac{\rho_0}{2} G_s(x_0, x) + \sigma_1 G_s(0, x) + \sigma_2 G_s(l, x) ; \\ \mathbf{I}_s(x) = \dfrac{\rho_0}{2} \mathbf{H}_s(x_0, x) + \sigma_1 \mathbf{H}_s(0, x) + \sigma_2 \mathbf{H}_s(l, x) , \end{cases} \qquad (12)$$

where ρ_0 is the time-averaged power being injected into the beam by the point force, σ_1 and σ_2 are the magnitudes of the boundary sources at both ends of the beam (Fig. 2), and G_s and $\mathbf{H}_s$ are the energy and intensity solutions Eq. (3) for plane waves. As discussed in the previous section, the fluid coupling acts as damping on the beam and the loss factor η_{rad} from Eq. (4) is introduced in the solutions Eq. (3) which leads to

$$G_s(x_1, x_2) = \frac{e^{-(\eta_s + \eta_{rad})\omega |x_1 - x_2|/c_s}}{2c_s}$$

and

$$\mathbf{H}_s(x_1, x_2) = \frac{e^{-(\eta_s + \eta_{rad})\omega |x_1 - x_2|/c_s}}{2} \mathrm{sgn}(x_2 - x_1)\mathbf{x} , \qquad (13)$$

where c_s is the energy velocity of flexural waves, and $\mathbf{x}$ is the unit vector oriented from left to right along the beam as shown in Fig. 2.

The acoustic energy $W_a(M)$ at any point M is described using Eq. (4) with no direct contribution since there is no acoustic source present,

$$W_a(M) = \int_0^l \sigma_{rad}(P, \mathbf{u}_{PM}) G_a(P, M)\, dP , \qquad (14)$$

where $\sigma_{rad}(P, \mathbf{u}_{PM})$ is the acoustic boundary source located at the point P and radiating in the direction $\mathbf{u}_{PM}$. The point P belongs on the beam, $0 < x < l$. G_a is the energy solution Eq. (3) for cylindrical waves

$$G_a(P, M) = \frac{e^{-\eta_a \omega PM/c_a}}{2\pi c_a PM} , \qquad (15)$$

where η_a is the damping loss factor of the fluid.

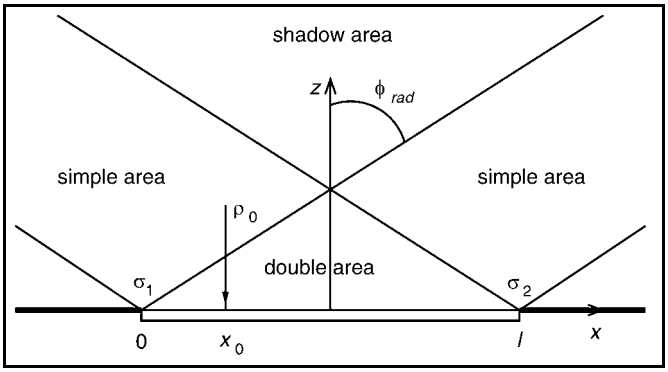

Figure 2. Energy flow formulation: notations and predicted pattern of the radiated field. σ_1, σ_2 and ρ_0 are the three sources providing power for the beam.

3.3. Solution of the Coupled System

The beam problem is solved first. Simply-supported boundary conditions for the beam imply that the structural intensity vanishes at both ends, $\mathbf{I}_s(0) = \mathbf{I}_s(l) = \mathbf{0}$. Using Eq. (12) for $\mathbf{I}_s$, the boundary source magnitudes σ_1, σ_2 are found to be

$$\sigma_1 = \frac{\rho_0}{2} \frac{e^{-(\eta_s + \eta_{rad})\omega x_0/c_s}}{1 - e^{-2(\eta_s + \eta_{rad})\omega l/c_s}} \quad \text{and} \quad \sigma_2 = \frac{\rho_0}{2} \frac{e^{-(\eta_s + \eta_{rad})\omega (l - x_0)/c_s}}{1 - e^{-2(\eta_s + \eta_{rad})\omega l/c_s}} . \qquad (16)$$

For a transverse force F applied at the beam axis location x_0, ρ_0 is usually calculated according to the relationship $\rho_0 = F^2 k_s/(8 m_s \omega)$ which represents the infinite in vacuo beam injected power.

In order to solve the acoustic medium problem, one needs to express the boundary sources σ_{rad} of Eq. (14). The directivity of these sources depends on the direction of propagation of the flexural energy as shown in the previous section. Consequently, the integral Eq. (14) is split into two terms corresponding to each propagation direction. Quantities due to the propagation from left to right are noted with a superscript + and from right to left with a superscript −. The radiated power within the angle $+\phi_{rad}$ defined in Eq. (7) is due to the flexural energy $W_s^+(x) = \rho_0/2\, G_s(x_0, x) Y(x - x_0) + \sigma_1 \times G_s(0, x)$ travelling from left to right, and the radiated power within the angle $-\phi_{rad}$ is due to the flexural energy $W_s^-(x) = \rho_0/2\, G_s(x_0, x) Y(x_0 - x) + \sigma_2 G_s(l, x)$ travelling from right to left. In these relationships, $Y(x)$ is the Heaviside step function and $W_s(x) = W_s^+(x) + W_s^-(x)$.

Due to the single angle of radiation, the directivity of the acoustic boundary sources $\sigma_{rad}^{\pm}(P, \mathbf{u}_{PM})$ is expressed in terms of a Dirac function, $\delta(\phi \mp \phi_{rad})$ where ϕ denotes the angle between the normal to the beam and the vector $\mathbf{u}_{PM}$. One may thus write $\sigma_{rad}^{\pm}(P, \mathbf{u}_{PM}) = \sigma_{rad}^{\pm}(P)\delta(\phi \mp \phi_{rad})$. The radiated power from Eq. (10) is equal to the integral of the intensity emanating from the source $\sigma_{rad}^{\pm}(P, \mathbf{u}_{PM})$ through a half circle of radius $\in$,

$$P^{\pm}_{rad}(P) = \int_{-\pi/2}^{\pi/2} \sigma^{\pm}_{rad}(P)\delta(\phi \mp \phi_{rad})H_a(\in)\in d\phi \,, \qquad (17)$$

where $H_a = c_a G_a$ with G_a coming from Eq. (15). When $\in$ tends to 0, the magnitude of the boundary sources is obtained, $P^{\pm}_{rad}(P) = \sigma^{\pm}_{rad}(P)/2\pi$. Then, using Eq. (10), expressions for $\sigma^{\pm}_{rad}(P)$ are derived, $\sigma^{\pm}_{rad}(P) = 2\pi\eta_{rad}\omega W^{\pm}_s(P)$ and the acoustic energy density Eq. (14) becomes

$$W_a(M) = \int_0^l 2\pi\eta_{rad}\omega W^{+}_s(P)\delta(\phi - \phi_{rad})G_a(P,M)dP +$$

$$\int_0^l 2\pi\eta_{rad}\omega W^{-}_s(P)\delta(\phi + \phi_{rad})G_a(P,M)dP \,. \qquad (18)$$

Using the geometrical relationship, $d\phi/\cos\phi = dP/MP$ for changing dP by $d\phi$, and substituting Eq. (15) for G_a, the integral Eq. (18) becomes

$$W_a(M) = \int_{\phi(0,M)}^{\phi(l,M)} \eta_{rad}\omega W^{+}_s(P)\frac{e^{-\eta_a\omega PM/c_a}}{c_a\cos\phi}\delta(\phi - \phi_{rad})d\phi +$$

$$\int_{\phi(0,M)}^{\phi(l,M)} \eta_{rad}\omega W^{-}_s(P)\frac{e^{-\eta_a\omega PM/c_a}}{c_a\cos\phi}\delta(\phi + \phi_{rad})d\phi \,, \qquad (19)$$

where $\phi(0,M)$ and $\phi(l,M)$ denote the angles between the normal to the beam and the vectors from each end of the beam to the point M. Considering the Dirac functions, both integrals become discrete,

$$W_a(M) = \eta_{rad}\omega W^{+}_s(P^{+})\frac{e^{-\eta_a\omega P^{+}M/c_a}}{c_a\cos\phi_{rad}} +$$

$$\eta_{rad}\omega W^{-}_s(P^{-})\frac{e^{-\eta_a\omega P^{-}M/c_a}}{c_a\cos\phi_{rad}}. \qquad (20)$$

P^+ denotes the only point of the beam that radiates towards M within the angle $+\phi_{rad}$ and P^- within the angle $-\phi_{rad}$. These points P^+ and P^- may be located within or outside the limits of the beam. In the latter case, their respective energy contribution must cancel in Eq. (20).

A geometrical analysis of this situation shows that the acoustic medium is separated into three areas as shown in Fig. 2. The double area is the area where M is affected by both flexural waves + and −; both points P^+ and P^- are located within the limits of the beam. The simple areas include beams of rays radiated from one wave. Finally, no radiated ray reaches any point M in the shadow areas, both points P^+ and P^- being located outside the limits of the beam. Furthermore, when the radiating point is located on the left of the excitation point, $x < x_0$, then W^+_s is due to the left boundary source σ_1 only, and W^-_s is due to both the right boundary source σ_2 and the direct source ρ_0. When the radiating point is located on the right of the excitation point, $x > x_0$, then W^+_s is due to both the left boundary source σ_1 and the direct source ρ_0, and W^-_s is due to the right boundary source σ_2 only. These steps in the energies W^+_s and W^-_s are responsible for some additional discontinuities in the acoustic field within the single and double areas.

4. NUMERICAL SIMULATIONS

Numerical results from both the solution of the equations of motion and the integral energy flow formulation are now compared. Assume a beam 1 metre long, excited by a transverse force of 1 N at the beam axis location $x_0 = 0.25$ m. The frequency is above the critical frequency of the fluid-loaded beam ($\omega/\omega_c = 3.4$) and there are about 30 flexural wavelengths along the beam. The structure is undamped ($\eta_s = 0$) in order to emphasise the energy exchanges between the beam and the fluid. The fluid is also undamped ($\eta_a = 0$). The ratio of the fluid density to the mass per unit length of the beam is $m_a/m_s = 8,6\,\mathrm{m}^{-1}$.

Energy flow results are compared with exact results averaged over one-third octave frequency bands. The exact results are obtained with a direct numerical simulation. The classical governing equations for a fluid-loaded beam with a continuity condition at the interface have been solved with a collocation method applied to the attached boundary formulation. No physical assumption has been introduced to simplify the problem. The Green's function involved for the acoustic pressure verifies the baffle condition outside the beam so that it is necessary just to discretise the beam. Indeed, this direct numerical simulation was computationally expensive. This is the reason why we have limited this study to a two-dimensional problem.

Figure 3 shows the averaged energy density along the beam. The thin line results from the solution of the equations of motion while the bold lines come from the energy flow calculation using Eqs. (12) and (16). The energies W^+_s propagating from left to right (dashed line) and W^-_s from right to left (dotted line) are also plotted.

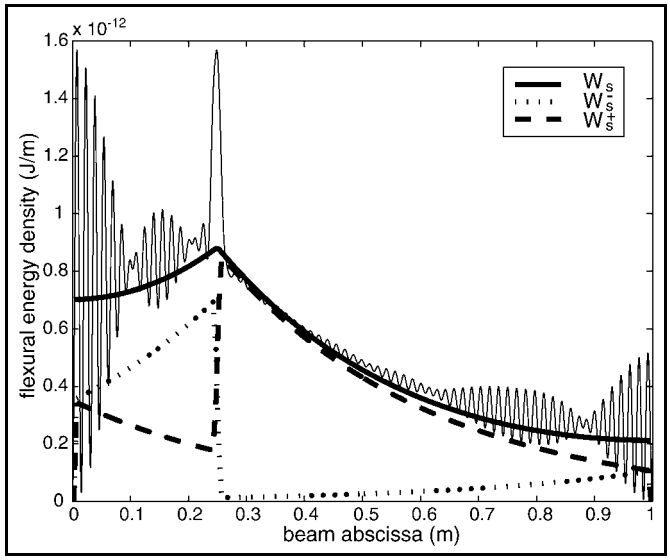

Figure 3. Flexural energy density in the beam, by solving equations of motion with thin lines, and by the energy flow approach with bold lines. Energy flow results for energies travelling in each direction are plotted with bold dashed and dotted lines. The excitation is located at the beam axis location $x_0 = 0.25$ m.

The decrease of these energies is due to losses produced by the radiation. The good agreement between the two calculations proves that the fluid coupling effects on the structural energy behaviour have been taken into account well by the energy flow approach.

In Fig. 4 the maps of the acoustic energy field obtained by the two calculations are shown. The energy flow solution is based on Eq. (20). The beam is located at $z = 0\,\text{m}$, between the beam axis values $x = -0.5\,\text{m}$ and $x = 0.5\,\text{m}$. The structural excitation in the frame of the acoustic medium is located at the beam axis location $x = -0.25\,\text{m}$. Several distinct areas of sound radiation can be identified clearly on both maps. Energy levels inside each area depend on the spatial variations of the flexural energies. This explains the two lines of discontinuity emanating from the excitation point (at the beam axis location $x = -0.25\,\text{m}$ on these maps) and due to discontinuities in the flexural energies W_s^+ and W_s^- at x_0 (see Fig. 3).

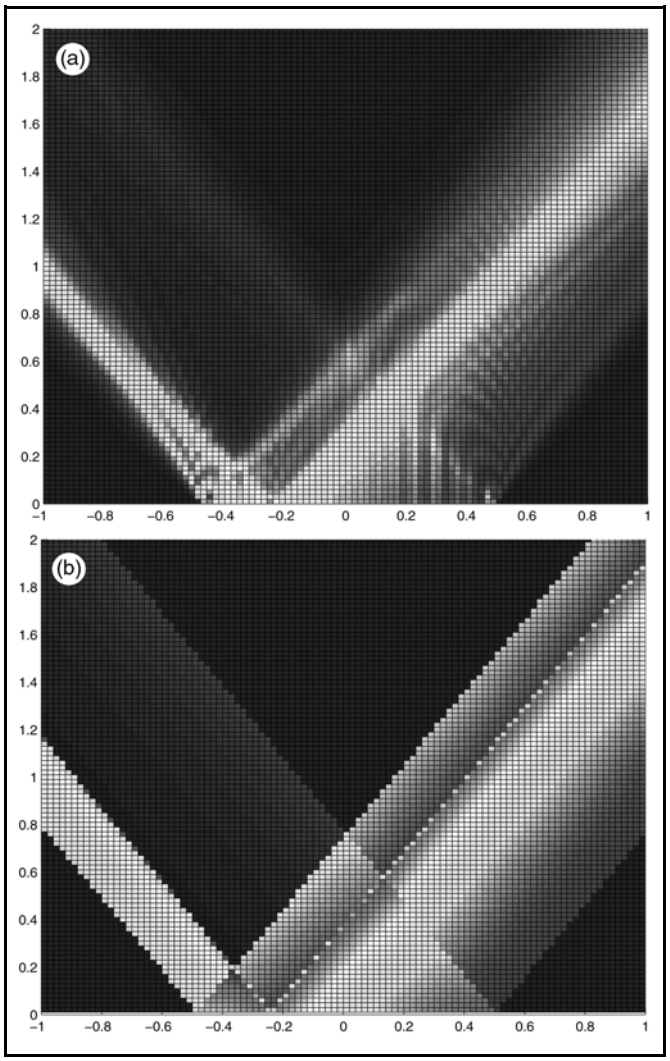

Figure 4. Acoustic energy density maps by solving equations of motion (a) and by the energy flow approach (b). The beam is located at $z = 0\,\text{m}$, between beam axis locations $x = -0.5\,\text{m}$ and $x = 0.5\,\text{m}$. The structural excitation in the present graphs is located at the beam axis location $x = -0.25\,\text{m}$.

Figures 5-7 compare values of the acoustic energy along lines parallel to the beam, at $z = 0.1\,\text{m}$, $z = 0.4\,\text{m}$ and $z = 1\,\text{m}$. The results obtained from the solution of the equations of motion are plotted with thin lines, while energy flow results are plotted with bold lines. Good agreement between the results of the two calculations is observed and the interpretation of energy variations may be easily performed in terms of radiated areas predicted by the energy flow formulation. In particular, the several discontinuities and variations in the acoustic energy are simply explained using the flexural energy variations of Fig. 3.

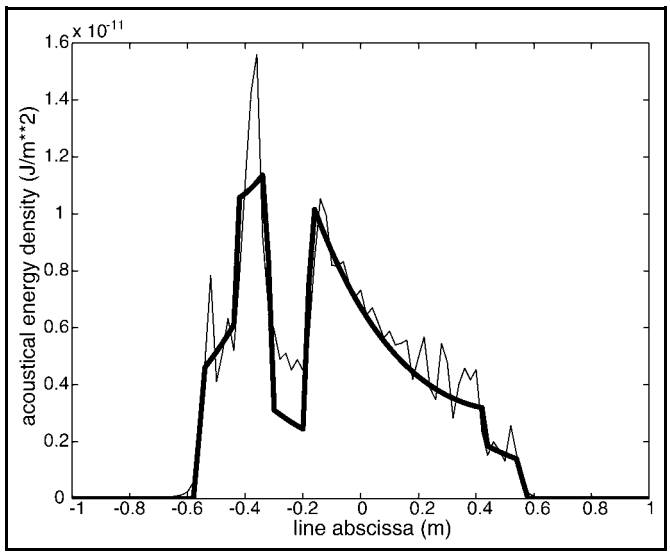

Figure 5. Acoustic energy along the line parallel to the beam at $z = 0.1\,\text{m}$. The result from the solving of equations of motion is plotted with the thin line while the energy flow result is plotted with the bold line.

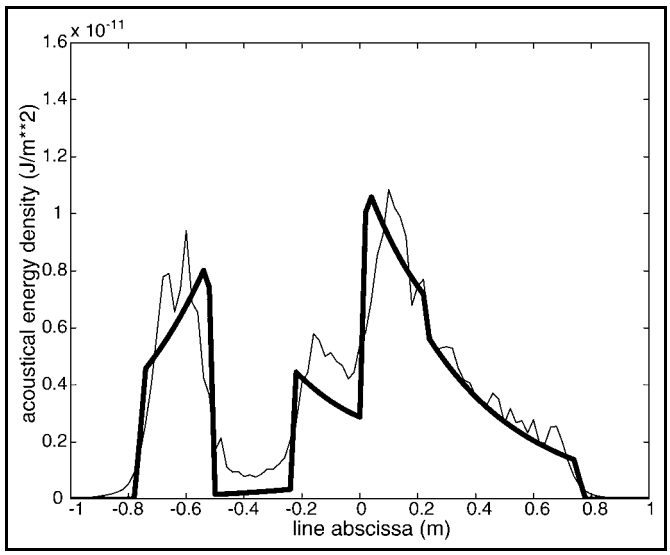

Figure 6. Acoustic energy along the line parallel to the beam at $z = 0.4\,\text{m}$. The result from the solving of equations of motion is plotted with the thin line while the energy flow result is plotted with the bold line.

5. CONCLUSIONS

The integral energy flow method has been investigated for structure-acoustic coupling above the critical frequency. The approach is based on two main assumptions: firstly, vibration fields are composed of travelling waves. This means that evanescent and inhomogeneous waves are not considered, which limits our study to the cases of light fluid loading. Furthermore, this implies that the energy fields are incorrectly described near discontinuities. Secondly, waves are assumed to be uncorrelated, which corresponds to a high frequency assumption.

For the simple case of an elastic beam radiating in a two-dimensional acoustic medium, the energy flow approach is shown to give the frequency-averaged values of the exact energy fields. By use of realistic directivities of power sources,

non-diffuse flexural and acoustic energy fields are spatially described and the energy flow analysis provides a simple explanation of the pattern of the radiated acoustic energy field.

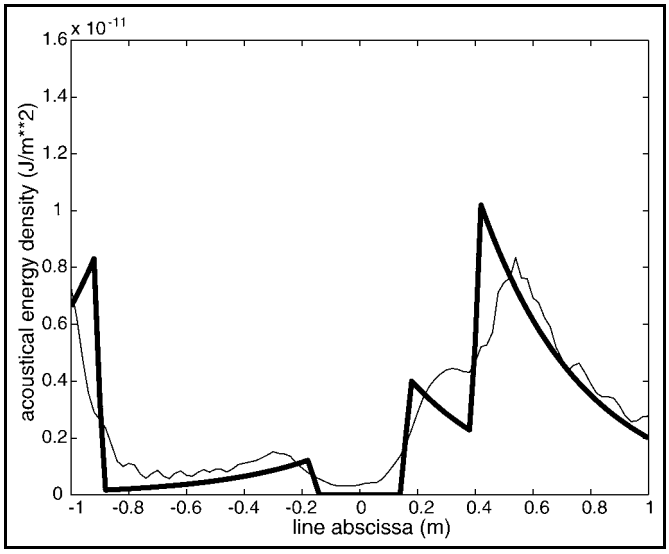

Figure 7. Acoustic energy along the line parallel to the beam at $z = 1$ m. The result from the solving of equations of motion is plotted with the thin line while the energy flow result is plotted with the bold line.

Although the present study is performed on a simple canonical problem, one must stress that the energy flow approach is easily applicable to more complex systems[13,14] (in particular, three-dimensional geometries). The acoustic radiation of vibrating structures below the critical frequency is due to diffraction effects that may be accounted for by the energy flow approach[15]. These diffraction effects occur above the critical frequency too, but they have been neglected in this analysis because they are far less efficient than the radiation from supersonic flexural waves. However, they may be important to predict acoustic energy fields in shadow areas, for example.

ACKNOWLEDGEMENTS

The authors gratefully acknowledge P. Nicot, E. Garrigues and D. Trentin from Dassault Aviation, France, for their scientific, technical and financial support.

REFERENCES

[1] Lyon R.H, and DeJong, R.G. *Theory and Applications of Statistical Energy Analysis*, Butterworth-Heinemann, USA, (1995).

[2] Crocker, M.J., and Price, A.J. Sound Transmission Using Statistical Energy Analysis, *Journal of Sound and Vibration*, **9** (3), (1969).

[3] Huff, J.E., and Bernhard, R.J. Prediction of High Frequency Vibrations in Coupled Plates Using Energy Finite Elements, *Proc. Inter-Noise*, (1995).

[4] Le Bot, A., and Cotoni, V. Boundary Element Method for Rays in Plates, *IMAC - XIX*, *Kissimmee*, 6-8 February, (2001).

[5] Kuttruff, H. Energetic Sound Propagation in Rooms, *Acustica*, **83**, (1997).

[6] Le Bot, A. A Vibroacoustic Model for High Frequency Analysis, *Journal of Sound and Vibration*, **211** (4), (1998).

[7] Le Bot, A., and Bocquillet, A. Comparison of an Integral Equation on Energy and the Ray-tracing Technique in Room Acoustics, *Journal of Acoustical Society of America*, **108** (4), (2000).

[8] Bitsie, F., and Bernhard, R.J. Structure-borne Noise Predictions Using an Energy Finite Element Method, *Proc. 1997 Noise and Vibration Conference*, Society of Automotive Engineers, (1997).

[9] Bernhard, R.J., and Huff, J.E. Structural-acoustic Design at High Frequency Using the Energy Finite Element Method, *Journal of Vibration and Acoustics*, **121**, (1999).

[10] Bouche, D., Molinet, F., and Mittra, R. *Asymptotic Method in Electromagnetics*, Springer-Verlag, (1997).

[11] Morse, P.M., and Ingard, K.U. *Theoretical Acoustics*, McGraw-Hill, (1968).

[12] Crighton, D.G. The Free and Forced Waves on a Fluid-loaded Elastic Plate, *Journal of Sound and Vibration*, **63** (2), (1979).

[13] Cotoni, V., Le Bot, A., and Jezequel, L. Vibroacoustique Hautes Frequences: Module Energetique Local Poue le Rayonnement, *Canadian Acoustic - Acoustique Canadienne, Proc. Of Acoustics Week in Canada*, **28** (3), (2000).

[14] Cotoni, V., Le Bot, A., Ichchou, M.N., and Jezequel, L. Line Excited Curved Panels Radiation at High Frequency by Power Flow Method, *Proc. Novem 2000 - Lyon*, 31 August - 1 September, (2000).

[15] Cotoni, V., Le Bot, A., and Jezequel, L. High Frequency Plate Radiation by Power Flow Analysis with Experimental Validation, *Proc. Inter-Noise 2000 - Nice*, 27-30 August, (2000).